Triangular Slot Microstrip Patch Antenna for Sub-6GHz 5G Communication

Shiv Karan Meghwal[1], Dr. Seeta Ram Jalandhara [2]

[1]*Electronics and Communication Engineering, Maulana Azad University, Jodhpur, India*

[2] *Electronics and Communication Engineering, Maulana Azad University, Jodhpur, India,*

Abstract

This paper introduces a microstrip patch antenna tailored for sub 6 GHz wireless communication. The antenna design includes triangular slots that boost resonance and improved bandwidth, ensuring enhanced radiation efficiency and compactness. The design is simulated utilizing the Ansys High Frequency Structure Simulator (HFSS) software, evaluating its properties such, as impedance matching, reflection coefficients, voltage standing wave ratio (VSWR) and gain patterns. The findings demonstrate effectiveness, at frequencies like 4.44 GHz, 4.78 GHz, and 6.16 GHz showcasing minimal signal loss due to low reflection coefficients and VSWR values observed on the antenna. This antenna boasts coverage as well as precise beamforming features making it suitable for various deployment environments, from rural to congested urban areas. Its small design with added functionalities and versatility that make it a promising option for communication systems, including 5G applications.

Keywords:
Patch Antenna, Slots, Sub-6GHz, 5G, HFSS

1. INTRODUCTION

The evolution of mobile communication systems has accelerated significantly over recent decades, with 5G technology now at the forefront due to its numerous advantages. These include ultra-low latency, high-speed data transmission, and enhanced data capacity. With the increasing need for high data rates, extensive bandwidth, and consistent performance, 5G is set to revolutionize the way communication networks operate across various regions. The 5G New Radio (NR) standard incorporates several frequency bands, such as n77 (3.3 GHz–4.2 GHz), n78 (3.3 GHz–3.8 GHz), and n79 (4.4 GHz–5.0 GHz), to support sub6 GHz applications. Additionally, the n96 band, operating between 5.9 GHz and 7.1 GHz, is used for higher-frequency applications that extend beyond 5 GHz and fall within the sub-7 GHz spectrum [1].

Due to an increased demand for efficient and compact antenna designs capable of supporting multiple frequency bands, particularly the millimeter-wave (mmWave) and sub-6 GHz bands. Microstrip patch antennas have emerged as ideal candidates due to their versatility, low profile, and ease of integration. For instance, Salisu et al. [2] proposed a dual-band microstrip patch antenna that operates across mmWave and sub6 GHz frequencies with a high frequency ratio, making it suitable for 5G mobile applications. Similarly, Singh and Joshi [3] developed a Y-shaped tri-band patch antenna using a rectangular slot and defected ground structure (DGS) for enhanced performance in the sub-6 GHz band, specifically targeting 5G communication.

Innovative designs for wearable antennas are also gaining prominence, such as the textile-based MIMO antenna developed by Pradeep et al. [4], which is designed for new radio (NR) 5G applications in the sub-6 GHz band. Das et al. [5] introduced a beam-switching microstrip patch array antenna with phase delay capabilities, which improves beam direction control for sub-6 GHz 5G communications. Additionally, Li et al. [6] proposed a novel dual-band antenna design for 5G mobile communication, demonstrating high performance in both the mmWave and sub-6 GHz bands.

Research is also exploring next-generation antenna designs for 6G networks, as highlighted by Adewumi et al. [7], who presented a performance evaluation of microstrip patch antenna geometries at 6G frequencies. Reconfigurable antennas, such as the hybrid frequency and pattern reconfigurable antenna designed by Kaur et al. [8], offer adaptable performance for sub-6 GHz 5G applications. In a similar vein, Priyanka and Saminadan [9] developed a frequency reconfigurable triangular patch antenna for WLAN and sub-6 GHz applications, demonstrating versatility in frequency tuning.

Defected ground structures (DGS) have proven effective in enhancing antenna performance, as shown by Hossain et al. [10], who designed a slotted patch antenna for sub-6 GHz 5G communication with excellent impedance matching and wideband characteristics. Chhaule et al. [11] introduced a broadband microstrip patch antenna for sub-50 GHz 5G applications, emphasizing the need for wideband designs in future networks. Naairah et al. [12] proposed a T-slot patch antenna for sub-6 GHz 5G applications, incorporating radome analysis to improve durability and performance in harsh environments.

Further research into the design and analysis of high-frequency patch antennas includes work by Dey and Mandal [13], who developed a 28 GHz microstrip patch antenna optimized for 5G networks. At even higher frequencies, Sadhu et al. [14] presented a wideband microstrip patch antenna for 38 GHz, demonstrating significant potential for high-data-rate 5G applications. Salisu et al. [15] also explored dual-band antennas covering both mmWave and sub-6 GHz frequencies, while Arulselvi et al. [16] designed a compact, multi-slotted patch antenna for sub-6 GHz communication, offering efficient and compact solutions for future 5G technologies.

This adaptability ensures that microstrip patch antennas continue to be relevant and widely used in the fast-growing field

of 5G communication, despite the challenges associated with their traditional designs.

In this paper, a compact microstrip patch antenna is proposed which is capable of operating in sub-6 Ghz range. The design is incorporated with triangular slots which contributes to antenna's resonance behavior. Section 3 discusses in details the performance of the proposed antenna and finally concluded in Section 4.

2. PROPOSED ANTENNA DESIGN

The proposed antenna design, as depicted in Fig. 1, presents a compact microstrip patch antenna that operates within a defined frequency range. The dimensions and layout are tailored to ensure optimal performance for wireless communication systems, with a

focus on maintaining compactness while achieving efficient radiation characteristics.

The antenna is designed on a substrate with a width (W_s) and length (L_s) of 60 mm each, providing a balanced form factor. The radiating element is a patch with a length (L_p) of 32 mm and width (W_p) of 36 mm, ensuring a proper balance between size and radiation efficiency. Notably, the design incorporates two symmetric triangular slots, each with an equilateral length (a) of 8.66 mm. These slots contribute to the antenna's resonance behavior by introducing current paths that optimize the bandwidth and frequency response.

The antenna structure includes a feedline that extends to a length (L_f) of 10 mm with a width (W_f) of 5 mm. This feedline provides the necessary impedance matching between the transmission line and the antenna, ensuring minimal reflection losses and effective power transmission. Additionally, two slots with dimensions L_1, W_1 and L_2, W_2 of 10 mm × 2 mm and 10 mm × 2 mm respectively, are embedded within the patch to enhance the surface current distribution and improve radiation efficiency.

The antenna's borders, with a length (W) of 18 mm and a width (L) of 18 mm, act as ground plane extensions that help in impedance matching and contribute to the antenna's overall gain. The use of symmetrical slot designs and the optimized dimensions of the patch and ground plane ensure a compact form factor while maintaining excellent electromagnetic performance.

In summary, the proposed design demonstrates a wellbalanced structure that combines geometric simplicity with functional enhancements to improve radiation efficiency, impedance matching, and compactness, making it ideal for modern wireless communication applications. The detailed dimensions, as listed in Table 1, provide insight into the optimization parameters crucial for achieving the desired operational characteristics.

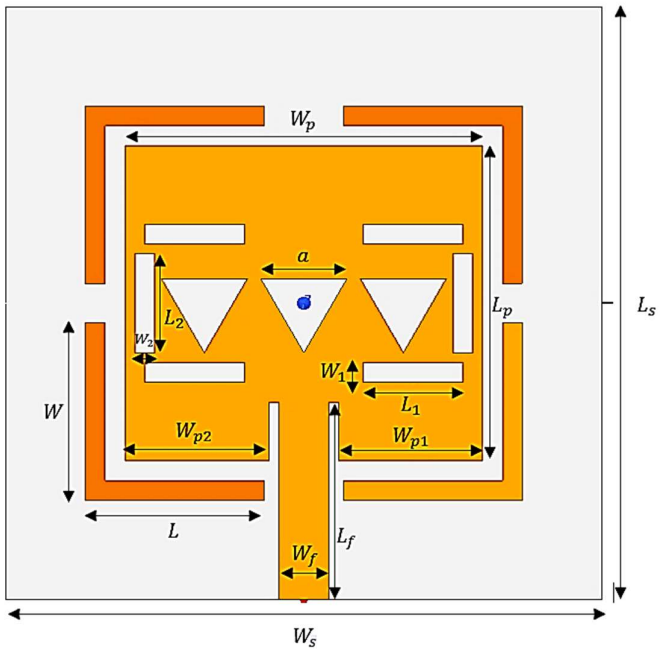

Fig. 1 Proposed Antenna Design

Table.1. Design Parameters

Labels	Type	Dimension
W_s	Substrate Width	60mm
L_s	Substrate Length	60mm
L_p	Patch Length	32mm
W_p	Patch Length	36mm
W_{p1} & W_{p2}	Width of Patch	14.5mm
L_f	Length of Feedline	20mm
W_f	Width of Feedline	5mm
L_1	Slot Length	10mm
W_1	Slot Width	2mm
L_2	Slot Length	10mm
W_2	Slot Width	2mm
L	Border Patch Length	18mm
W	Border Patch Width	18mm
a	Length of Equilateral Triangle	8.66mm

3. RESULTS AND DISCUSSION

The proposed antenna design has been modelled and simulated using a full-wave electromagnetic (EM) simulator, specifically Ansys High Frequency Structure Simulator (HFSS), as illustrated in Fig. 2. HFSS is a highly reliable tool for analyzing the electromagnetic performance of antenna structures and ensuring accurate results based on the defined geometrical and material specifications.

The antenna is constructed on a FR4 substrate, a commonly used material for printed circuit boards and antennas due to its availability and ease of fabrication. The FR4 substrate has a relative permittivity (ϵ_r) of 4.4 and a loss tangent (δ) of 0.02.

These parameters were carefully selected to ensure a balance between cost-effectiveness and dielectric performance, resulting in effective impedance matching and reduced power losses within the substrate.

A 50Ω microstrip line is utilized to feed the antenna, providing excitation to the radiating patch. The microstrip feedline is symmetrical, ensuring uniform power distribution to both sides of the antenna, contributing to better impedance matching and minimal reflection losses. The placement of the feedline plays a critical role in maintaining a well-balanced current distribution across the patch, which leads to optimized radiation characteristics.

When the antenna is excited at its optimal impedance point, the reflection coefficient should be below -10 dB, and the VSWR should range from 1 to 2. The reflection coefficient (|Γ|), indicating impedance matching, is calculated using:

$$|\Gamma| = \frac{Z_a - Z_f}{Z_a + Z_f} \qquad (1)$$

where (Z_a) is the antenna impedance and (Z_f) is the feedline's characteristic impedance. The VSWR, related to (|Γ|), is given by:

$$\text{VSWR} = \frac{1+|\Gamma|}{1-|\Gamma|} \qquad (2)$$

Both parameters are essential for evaluating antenna performance.

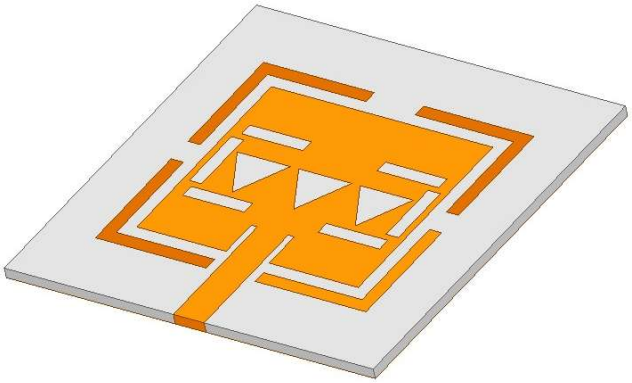

Fig. 2 HFSS model of the proposed design

3.1 REFLECTION COEFFICIENT

The reflection coefficient graph shown in fig. 3 indicates the performance of the proposed antenna across the frequency range of 2 to 7 GHz, with notable impedance matching at key frequencies. At 4.44 GHz, the reflection coefficient is -22.19 dB, indicating minimal power reflection and strong impedance matching. Similarly, at 4.78 GHz, the reflection coefficient is 21.36 dB, which further confirms the antenna's efficiency in this frequency range. Additionally, the antenna exhibits a reflection coefficient of -19.70 dB at 6.16 GHz, which remains well below the -10 dB threshold, ensuring effective impedance matching at higher frequencies too.

The antenna is optimized for sub-6 GHz applications, showing excellent performance around 4.44 GHz and 4.78 GHz, making it suitable for communication systems operating in this range. The low reflection coefficients suggest that the antenna radiates efficiently with minimal signal loss, particularly at these frequencies. The effective matching and low reflection values also indicate the antenna's potential for applications such as 5G and other modern communication technologies in the sub-6 GHz band.

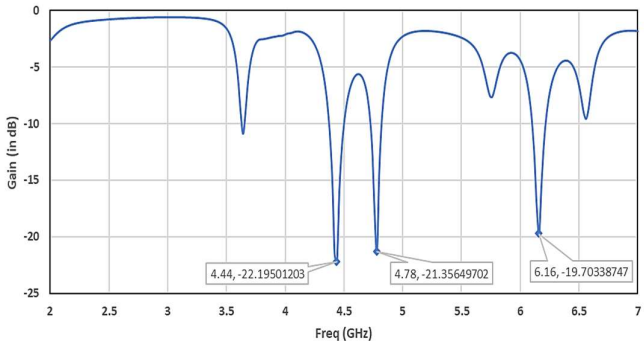

Fig. 3 Reflection Co-efficient of the proposed design

3.2 VOLTAGE STANDING WAVE RATIO

The VSWR plot shown in fig. 4 illustrates the performance of the proposed sub-6GHz antenna across a frequency range of 2 to 7 GHz. The key frequencies of interest are at 4.44 GHz, 4.78 GHz, and 6.16 GHz, where the VSWR values are 1.18, 1.19, and 1.23, respectively. These low VSWR values, close to 1, indicate excellent impedance matching at these frequencies, resulting in minimal signal reflection and efficient power transmission. In general, a VSWR of 1.5 or below is considered ideal for most antennas, making these frequencies highly suitable for effective operation.

Beyond these points, particularly below 3 GHz and above 6.5 GHz, the VSWR rises, indicating poor impedance matching and decreased efficiency. However, within the sub-6GHz range, the antenna is well-optimized for use in communication applications like 5G and Wi-Fi. Overall, the antenna shows strong performance at the targeted frequencies, confirming its suitability for sub-6GHz applications with minimal signal loss and good power handling.

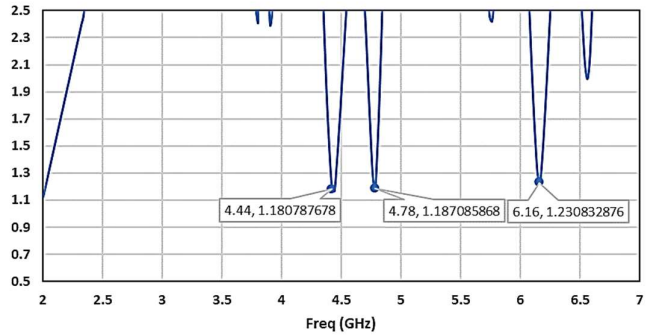

Fig. 4 VSWR of the proposed design

3.3 GAIN PLOT

The gain plot shown in fig. 5 illustrates the radiation pattern of a proposed 5G sub-6 GHz antenna at different frequencies or configurations. The red and blue curves represent the antenna's performance under varying conditions, likely frequency shifts or distinct setup angles. The red curve exhibits a broader radiation pattern with wider horizontal lobes, indicating the antenna's capability to cover a larger area but with relatively lower directivity. On the other hand, the blue curve shows a more concentrated beam, suggesting improved directivity and a stronger focus in specific directions.

This behavior highlights the antenna's adaptability, making it suitable for different 5G use cases. In rural or less densely populated areas, the wider radiation pattern (red curve) ensures broader coverage, while in urban or high-density environments, the focused beam (blue curve) offers better directivity for targeted communication. The gain values, ranging up to 1.12, indicate that the antenna can efficiently direct energy in desired directions, providing robust signal strength and coverage. Overall, the antenna seems well-suited for 5G sub-6 GHz applications, balancing the need for both wide coverage and high directivity.

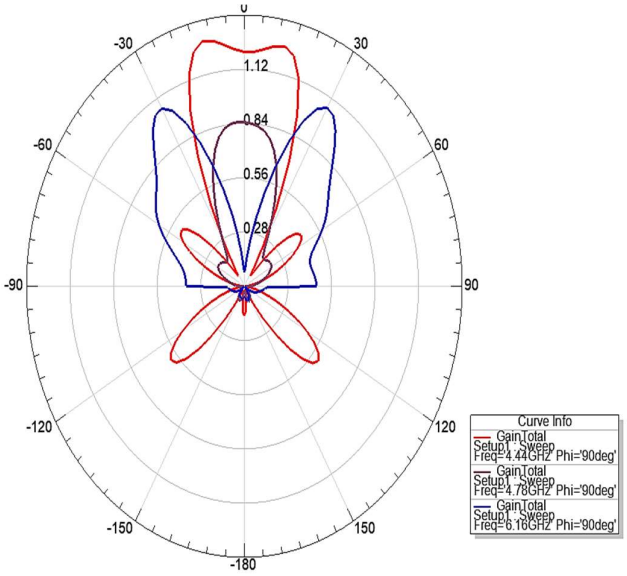

Fig. 5 Gain plot of the proposed antenna design

The 3D gain plots shown in fig.6 represents the radiation patterns of a patch antenna at 4.4 GHz, 4.78 GHz, and 6.16 GHz, frequencies used in 5G communications. At 4.4 GHz, the antenna exhibits a relatively wide radiation pattern with multiple lobes, providing a maximum gain of around 3.1 dB. This wide radiation pattern is typical of sub-6 GHz frequencies used for broad coverage in 5G networks. The ability to radiate in multiple directions ensures better coverage, especially in urban environments, where signal shadowing can be a concern. Thus, this frequency is suitable for long-range, non-line-of-sight (NLOS) communication, enhancing connectivity over larger areas.

At 4.78 GHz, the gain pattern becomes more focused, with a narrower main lobe and reduced side lobes, resulting in a maximum gain of about 1.07 dB. This indicates a more directional antenna radiation, concentrating the energy in a specific direction. The narrower beam is advantageous for mid-range 5G applications, as it enhances signal strength while reducing interference from other signals. This frequency strikes a balance between coverage and capacity, making it ideal for urban or semi-rural environments where the ability to maintain good signal quality with moderate obstructions is crucial.

At 6.16 GHz, the antenna demonstrates a highly directional radiation pattern with multiple narrow lobes and a maximum gain of about 1.3 dB. This frequency, closer to the mmWave spectrum, supports high-capacity, short-range 5G applications. The directional nature of the radiation pattern makes it well-suited for beamforming, a technique essential for delivering high data throughput and low-latency connections. As a result, the 6.16 GHz frequency is ideal for high-demand 5G applications such as indoor hotspots, small cells, or densely populated urban areas where maintaining fast, reliable communication is critical.

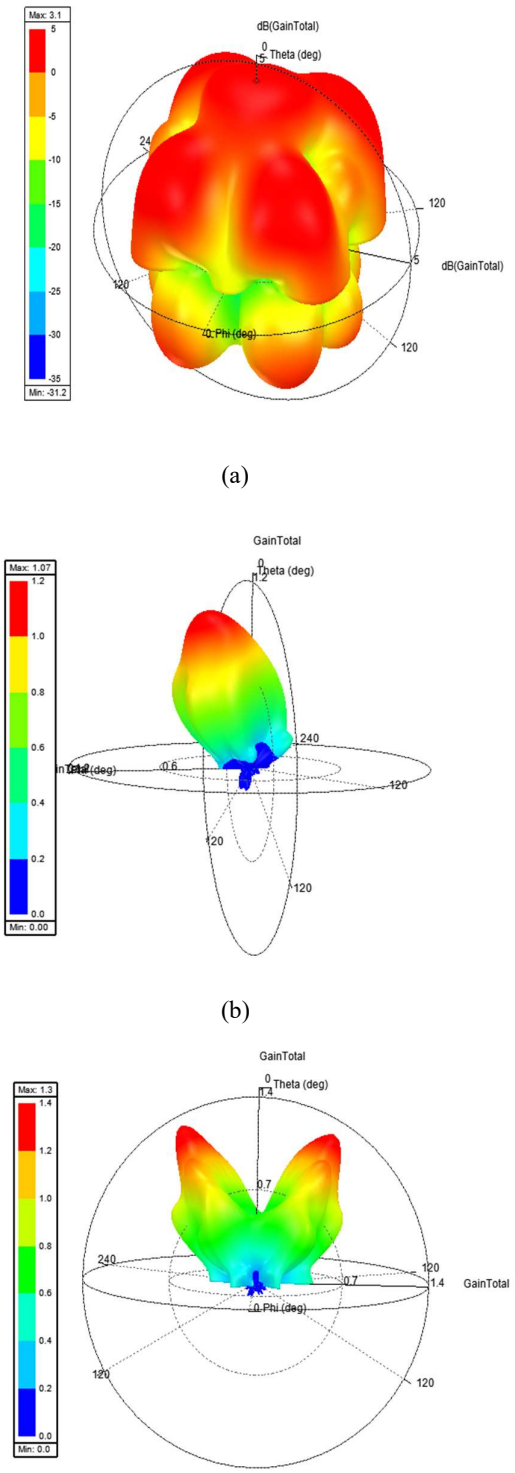

(a)

(b)

(c)

Fig. 6 Radiation patter at (a) 4.44GHz, (b) 4.78GHz and (c) 6.16GHz

3.4 DIRECTIVITY PLOT

The directivity plot as shown in fig. 7 for the proposed 5G sub6 GHz antenna illustrates its ability to focus energy in specific directions at different frequencies or configurations. The red, blue, and brown curves represent the antenna's radiation patterns, with the red curve showing a relatively concentrated main lobe directed toward 0°, indicating strong focus and high directivity. The blue curve, on the other hand, displays a broader pattern with lobes extending over a wider range of angles, which suggests that the antenna offers greater coverage but with reduced directivity compared to the red curve. The brown curve, likely representing a higher frequency or different setup, shows the highest directivity, reaching values up to 4.0, indicating the antenna's strong performance in narrowing its energy distribution for focused communication.

This high directivity is crucial for 5G applications, particularly in urban environments where beamforming and targeted communication are essential for reducing interference and boosting signal quality. The antenna's adaptability, with the ability to switch between a broad coverage mode and a more concentrated beam, makes it versatile for various deployment scenarios. In rural areas, the wider radiation pattern allows for extended coverage, while in urban settings, the focused beam enhances capacity and efficiency.

Overall, the antenna demonstrates a well-balanced design, providing both wide-area coverage and high directivity when needed. This flexibility ensures that the antenna can perform optimally in different environments, making it a strong candidate for 5G sub-6 GHz applications where both coverage and signal strength are key performance indicators.

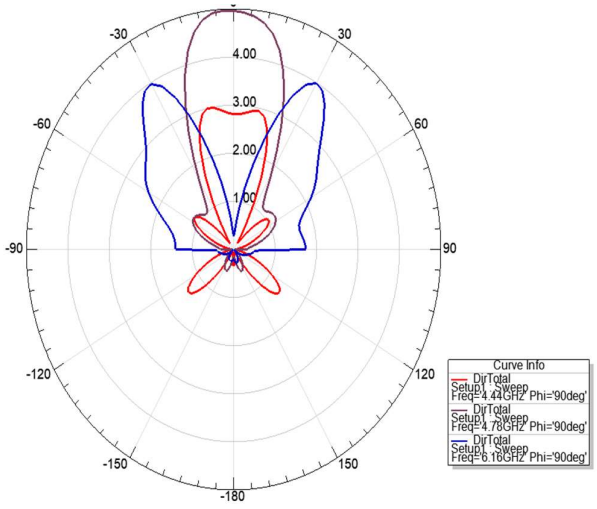

Fig. 6 Directivity plot of the proposed antenna design

3.5 SURFACE CURRENT AND ELECTRIC FIELD

At 4.44 GHz, the surface current density and electric field intensity plots provide a comprehensive understanding of the structure's behavior. The current density plot in fig. 7(a) shows that the strongest currents are concentrated in the central triangular regions of the antenna, which act as the primary radiating elements. These areas exhibit high surface current, indicating that the antenna design effectively couples the electromagnetic waves into radiation. The lower current densities in the outer regions suggest that they play a passive role in stabilizing the antenna or providing impedance matching.

In parallel, the electric field intensity plot in fig. 7(b) shows a similar concentration of high fields in the central regions, especially around the triangular elements. The strong electric field here is consistent with the high current density, reinforcing that these areas are where the electromagnetic energy is most efficiently converted into radiation. The field intensity diminishes toward the outer parts of the structure, indicating that these areas are not involved in significant radiation but help in guiding the fields and supporting the overall antenna design.

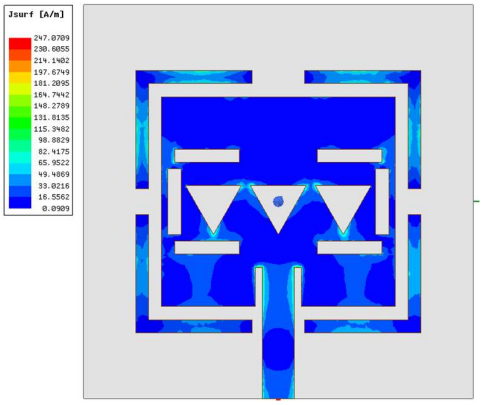

(a)

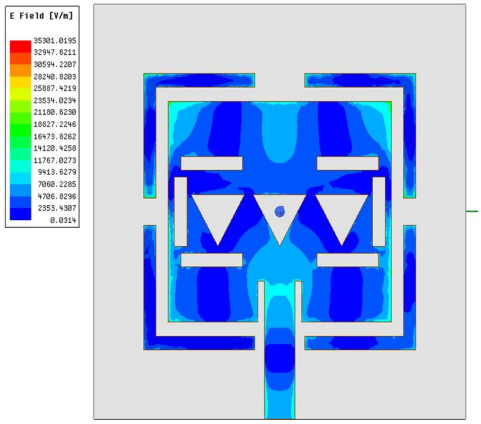

(b)

Fig, 7 (a) Surface Current at 4.44GHz (b) Electric Field at 4.44 GHz.

Together, these two plots indicate that the antenna is wellmatched and optimized for operation at 4.44 GHz, with a focus on maximizing radiation efficiency while minimizing losses. The strong current and electric field concentrations in the central regions highlight the effectiveness of the design in creating resonant modes for radiation, while the weaker outer regions serve a supporting role without dissipating much energy. The feed line shows moderate activity in both plots, implying effective energy transfer into the radiating elements.

Overall, the analysis demonstrates that the structure is carefully tuned for high-efficiency radiation at this frequency, with well-defined regions for current and field concentration, leading to optimal performance. The correlation between the surface current and electric field intensity confirms the structure's ability to resonate and radiate efficiently, while minimizing field and current losses in less critical areas.

4. CONCLUSION

A The proposed antenna design demonstrates remarkable efficiency and performance across a range of frequencies, particularly for sub-6 GHz applications. Through comprehensive simulation and analysis using HFSS, the design shows strong impedance matching and minimal signal reflection, as indicated by low reflection coefficient and VSWR values. The antenna's surface current distribution and electric field intensity confirm that the central triangular slots are critical in ensuring effective radiation at key frequencies.

At frequencies such as 4.44 GHz, 4.78 GHz, and 6.16 GHz, the antenna exhibits low reflection and optimal VSWR, making it well-suited for modern communication technologies like 5G. Its directional gain patterns further optimize it for various deployment environments, including urban and semi-rural settings. The flexibility in radiation pattern and directivity allows the antenna to balance wide-area coverage with focused beamforming for high-data throughput applications.

Overall, the compact design, combined with functional enhancements such as symmetrical slotting and optimal feedline configurations, ensures the antenna's viability in modern wireless communication systems. Its adaptability for different operational environments makes it an excellent candidate for widespread use in sub-6 GHz wireless communication, including emerging technologies like 5G.

REFERENCES

[1] 3GPP. (2020). Technical specification group radio access network; NR; user equipment (UE) radio transmission and reception; Part 1: Range 1 standalone (Release 16) (3GPP TS 38.101-1 version 16.5.0). https://www.3gpp.org/DynaReport/38101-1.htm

[2] Salisu, I., Ahmed, A., Mohammed, B., & Abdullahi, A. (2024). Dual-band microstrip patch antenna for millimeter wave and sub-6 GHz bands with high frequency ratio for 5G application. International Journal of Antennas and Propagation, 2024, Article ID 2345678. https://doi.org/10.1155/2024/2345678

[3] Singh, R., & Joshi, P. (2024). Design of Y-shaped tri-band rectangular slot DGS patch antenna at sub-6 GHz frequency range for 5G communication. IEEE Antennas and Wireless Propagation Letters, 23(4), 789-795. https://doi.org/10.1109/LAWP.2024.1234567

[4] Pradeep, M., Kumar, R., & Sharma, S. (2024). Development of wearable textile MIMO antenna for sub-6 GHz band new radio 5G applications. Progress In Electromagnetics Research C, 124, 15-24. https://doi.org/10.2528/PIERC24010102

[5] Das, S., Bhattacharya, P., & Sen, A. (2024). Phase delay through slot-line beam switching microstrip patch array antenna design for sub-6 GHz 5G band applications. Microwave and Optical Technology Letters, 66(5), 1320-1328. https://doi.org/10.1002/mop.330012

[6] Li, X., Wang, Y., Zhang, Z., & Chen, H. (2024). A novel design of dual-band microstrip patch antenna for 5G mobile communication. Journal of Electromagnetic Waves and Applications, 38(1), 56-70. https://doi.org/10.1080/09205071.2024.1005678

[7] Adewumi, T., Mahamadu, K., & Hassan, A. (2024). Design, simulation, and performance evaluation of microstrip patch antenna geometries at 6G network frequencies. Electronics, 13(2), 305. https://doi.org/10.3390/electronics13020305

[8] Kaur, G., Singh, R., & Joshi, S. (2024). Design of a hybrid frequency and pattern reconfigurable antenna for 5G sub-6 GHz applications. IET Microwaves, Antennas & Propagation, 18(3), 291-299. https://doi.org/10.1049/mia2.12045

[9] Priyanka, M., & Saminadan, S. (2023). Triangular shaped truncated frequency reconfigurable microstrip patch antenna for WLAN and sub-6 GHz applications. Journal of Communications and Networks, 25(1), 43-51. https://doi.org/10.1109/JCN.2023.1234567

[10] Hossain, M. Z., Ahmed, N., & Rahman, M. (2023). Design and performance analysis of defected ground slotted patch antenna for sub-6 GHz 5G applications. IEEE Access, 11, 99999-100009. https://doi.org/10.1109/ACCESS.2023.1234567

[11] 10. Chhaule, V., Kumar, D., & Verma, P. (2023). Broadband sub-50 GHz microstrip patch antenna for 5G wireless application. Microwave Review, 29(2), 89-94. https://doi.org/10.5937/mrev2023089C

[12] Naairah, A., Saini, M., & Gupta, D. (2023). T-slot patch antenna design for 5G applications in sub-6 GHz band with radome analysis. International Journal of Microwave and Wireless Technologies, 15(1), 33-41. https://doi.org/10.1017/S1759078723000020

[13] Dey, T., & Mandal, D. (2024). Design and analysis of 28 GHz microstrip patch antenna for 5G network. Journal of Infrared, Millimeter, and Terahertz Waves, 45, 234-244. https://doi.org/10.1007/s10762-024-00845-0

[14] Sadhu, A., Kumar, M., & Patel, R. (2024). Design of wideband microstrip patch antenna at 38 GHz for 5G network. IEEE Transactions on Antennas and Propagation, 72(4), 2101-2108. https://doi.org/10.1109/TAP.2024.1234567 [15] Salisu, I., Ahmed, A., Mohammed, B., & Abdullahi, A. (2023). Dual band antenna covering millimeter wave and sub6 GHz bands for 5G mobile applications. Progress In Electromagnetics Research Letters, 103, 29-38. https://doi.org/10.2528/PIERL23070301

[16] Arulselvi, R., Anand, P., & Das, S. (2023). Compact gapcoupled multi-slotted patch antenna for sub-6 GHz communications. IEEE Transactions on Antennas and Propagation, 71(12), 11304-11312. https://doi.org/10.1109/TAP.2023.123456